Journal of Solid State Chemistry 184 (2011) 2272–2277

Contents lists available at ScienceDirect

Journal of Solid State Chemistry

journal homepage: www.elsevier.com/locate/jssc

A high temperature diffraction-resistance study of chalcopyrite, $CuFeS_2$

T.E. Engin [a,b,1], A.V. Powell [a,*], S. Hull [b]

[a] Department of Chemistry, Perkin Building, Heriot-Watt University, Edinburgh, EH14 4AS, UK
[b] The ISIS Facility, STFC Rutherford Appleton Laboratory, Chilton, Didcot, OX11 0QX, UK

ARTICLE INFO

Article history:
Received 25 March 2011
Received in revised form
18 June 2011
Accepted 27 June 2011
Available online 2 July 2011

Keywords:
Neutron diffraction
Magnetism
Electrical properties
In-situ studies
Sulphides

ABSTRACT

The electrical, magnetic and structural properties of synthetic chalcopyrite, $CuFeS_2$, have been studied up to 873 K using DC resistance measurements performed in-situ during neutron powder diffraction experiments. Under ambient conditions the material adopts the accepted structural model for $CuFeS_2$ in the space group $I\bar{4}2d$, with the magnetic moment of the Fe^{3+} cations aligned along [001]. The electrical resistivity is around 0.3 Ω cm under ambient conditions, consistent with semiconductor character, and decreases slightly with increase in temperature until a more abrupt fall occurs in the region 750–800 K. This abrupt change in resistivity is accompanied by a structural transition to a cubic zinc blende structured phase (space group $F\bar{4}3m$) in which Cu^+ and Fe^{3+} cations are disordered over the same tetrahedral crystallographic sites and by a simultaneous loss of long-range magnetic order. The implications of these results are discussed in the context of previous studies of the chalcopyrite system.

1. Introduction

The most common naturally occurring ternary sulphide system is that containing copper, iron and sulphur. Minerals within the Cu–Fe–S system are found in nearly every geological environment and rock type and are well known from lunar and meteoritic materials [1]. Within this ternary system, chalcopyrite, $CuFeS_2$, is the principal source of the world's copper. $CuFeS_2$ is a magnetic semiconductor [2] and the structural prototype for a large class of compounds of general formula ABQ_2, including the important II–IV–V_2 (A=Be, Mg, Zn, Cd; B=C, Si, Ge, Sn and Q=N, P, As, Sb [3]) and I–III–VI_2 (A=Cu, Ag; B=Ga, In; Q=S, Se, Te [4]) materials. There has been a recent resurgence of interest in the chalcopyrite family of materials as dilute magnetic semiconductors. The opportunity to inject spins into a non-magnetic semiconductor, through the introduction of magnetic centres [5,6], offers the prospect of exploiting the correlation between charge and spin of the electron to create spintronics devices. The capacity to engineer band gaps has also led to interest in chalcopyrites as candidate materials for photovoltaic devices [7–9].

$CuFeS_2$ crystallises in the tetragonal space group $I\bar{4}2d$ and adopts a superstructure of the zinc blende crystal structure with the copper and iron cations ordered over alternate 4-coordinate sites. The structure may be described as an array of vertex linked CuS_4 and FeS_4 tetrahedra (Fig. 1). $CuFeS_2$ is an n-type direct-band-gap semiconductor. Band gaps of 0.5, 0.33 and 0.6 eV have been determined at room temperature for naturally occurring samples [10] and a value of 0.58 eV for thin-films grown in the laboratory [11]. However, electrical measurements reveal a complex temperature dependence to the transport properties [12]. The electrical conductivity increases on heating from 195 to 223 K, then falls, until at 573 K, a sharp increase in conductivity is observed. It was suggested this behaviour indicates that at temperatures below 223 K, the conductivity is dominated by extrinsic (impurity) conduction, whilst at higher temperatures intrinsic conduction dominates. A second further decrease in electrical conductivity at 773 K was reported by Boltaks and Tarnovskii [13], although this has not been observed by other workers. On cooling below T_N=823 K [14], $CuFeS_2$ undergoes a transition to a long-range antiferromagnetically ordered state. Whilst it was initially proposed [15] that the magnetic properties indicated a mixture of formal valence states for both copper and iron, Mössbauer [16,17] and photoelectron spectroscopic measurements [15,18] appear to confirm the formalism $Cu^+Fe^{3+}S_2$ and the presence of high-spin Fe^{3+}, although the alternative, $Cu^{2+}Fe^{2+}S_2$, has also been proposed on the basis of X-ray absorption data [19]. Pearce et al. [20] have suggested on the basis of X-ray photoemission and X-ray absorption data that assignment of formal valence states to copper sulphides may be an oversimplification in situations where there is appreciable covalency. There have also been several investigations of the temperature dependence of the crystal structure of $CuFeS_2$. A transition from the ambient temperature tetragonal structure to a cubic phase has been reported to occur on heating above 830 K [21], accompanied by disordering of the Cu^+ and Fe^{3+} cations

* Corresponding author. Fax: +44 131 451 3180.
E-mail address: a.v.powell@hw.ac.uk (A.V. Powell).
[1] Present address: Tubitak Ume, PO Box 54, 41470 Gebze Kocaeli, Turkey.

0022-4596/$ - see front matter © 2011 Elsevier Inc. All rights reserved.
doi:10.1016/j.jssc.2011.06.036

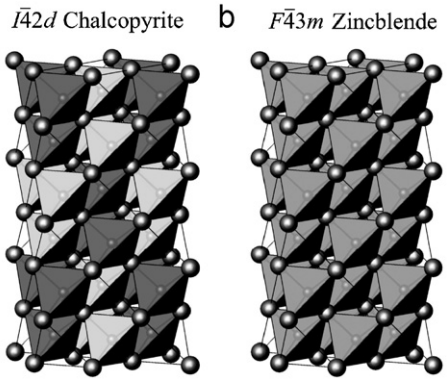

Fig. 1. Polyhedral representations of (a) the chalcopyrite and (b) the zinc blende crystal structures. In the former, tetrahedra containing Cu^{+} and Fe^{3+}, shown as light and dark coloured polyhedra, respectively, show long-range ordering. Large circles represent sulphide anions and small circles the transition-metal cations.

over the tetrahedral sites. Other workers [22] have suggested that decomposition to pyrite plus a cation-deficient zinc-blende-like phase ($Cu_{12}Fe_{11}S_{29}$) occurs on heating above the Néel temperature, whilst it has also been proposed that decomposition of the sample occurs below T_N [23].

Many of the investigations of chalcopyrite have been performed on naturally occurring samples. The attendant problems of uncertainties over sample composition and homogeneity, together with the presence of impurity phases such as FeS_2, may be contributory factors to the apparent deviations between measurements made in different laboratories on different samples. In an effort to understand the apparently conflicting reports of the structural, magnetic and electronic behaviours of chalcopyrite at high temperature, we have performed a powder neutron diffraction experiment on a synthetic sample of $CuFeS_2$. The sample was contained in a specially designed *in-situ* diffraction-resistance cell. This cell enables the structural, magnetic and electron-transport properties of a material to be investigated simultaneously, eliminating any possible differences that might arise when comparing results from samples of slightly different stoichiometry or measurements performed under differing conditions.

2. Experimental

$CuFeS_2$ was synthesised by direct reaction of a stoichiometric mixture of the pure elements (Fe, Cu and S, 99.95% Sigma-Aldrich) in a fused silica tube evacuated to $<10^{-4}$ Torr and sealed. The sealed tube was placed in a furnace and heated at 723 K for 7 days, prior to cooling at the natural rate of the furnace. The sample was then reground to homogenise it, prior to re-firing at 1173 K for 2 days. The sample was finally cooled to room temperature at 25 K h^{-1}. Following characterisation by powder X-ray diffraction (Supplementary Information), which confirmed the identity of the product phase, the powder was pressed into a cylindrical pellet (radius, $r=2.5$ mm; length, $l=10$ mm). The pellet was sintered in an evacuated sealed fused-silica tube for 7 days at 1146 K. This produced a mechanically robust shiny gold-coloured ingot.

The neutron diffraction measurements were performed on the POLARIS powder diffractometer at the ISIS facility, Rutherford Appleton Laboratory, U.K. [24], using the backscattering detector bank (covering scattering angles of $130^{\circ}<2\theta<160^{\circ}$, giving a d-spacing range of $0.2<d(\text{Å})<3.2$, with a resolution of $\Delta d/d\sim5\times10^{-3}$) and the low-angle bank ($28^{\circ}<2\theta<42^{\circ}$, $0.5<d(\text{Å})<8.3$, $\Delta d/d\sim10^{-2}$). The cylindrical ingot, held between two spring-loaded platinum contacts, was contained in an *in-situ* diffraction-resistance cell under an atmosphere of 0.5 bar of dry argon. Details of the construction and operation of this cell have been presented previously [25]. Powder neutron diffraction data were collected over the temperature range 398–873 K in 25 K steps. The sample temperature was allowed to equilibrate for 5 min prior to the collection of diffraction data over a period of approximately 30 min at each temperature. At a given temperature, during the period over which the neutron diffraction data were recorded, resistance measurements were made every 30 s. The electrical resistance of the sample was measured by the four-probe DC method using a Keithley series 2400 digital source metre. The value of resistivity, ρ, at each temperature was obtained by averaging the values of resistance, R, taken during the neutron diffraction data collection and converting to resistivity using the dimensions of the ingot, according to the expression, $\rho=\pi r^2 R_{ave}/l$. Analysis of the powder neutron diffraction data was carried out by the Rietveld method implemented in the GSAS suite of programs [26].

3. Results and discussion

The results of the neutron powder diffraction and *in-situ* resistivity study of $CuFeS_2$ are summarised in Fig. 2. The diffraction data obtained from the high-resolution backscattering detector bank (Fig. 2a) indicate the splitting of many of the Bragg reflections at temperatures close to ambient, consistent with the description of the chalcopyrite structure as a tetragonal superstructure of the cubic zinc blende type (Fig. 1a). At room temperature, all reflections, other than those arising from boron nitride of the *in-situ* diffraction-resistance cell, could be indexed on the basis of a tetragonal unit cell. At temperatures above *ca.* 800 K the peak splitting disappears, resulting in a simpler diffraction pattern that can be indexed on the basis of a cubic unit cell.

Ambient-temperature data from the low-angle detector bank (Fig. 2b), which accesses longer d-spacings, contain moderately intense peaks at $d=3.74$ and 4.72 Å. These may be indexed as the (110) and (101) reflections of a tetragonal unit cell of the same dimensions as that of the chalcopyrite structure. However, the former is systematically absent in space group $I\bar{4}2d$, whilst the latter is predicted to have an extremely low intensity (*ca.* 1% of I_{max}) for the chalcopyrite structural model. This suggests these reflections are magnetic in origin and the magnetic propagation vector $\mathbf{k}=(0,0,0)$. These longer d-spacing peaks disappear on heating above *ca.* 800 K, indicating the loss of long-range magnetic order is coincident with the transition to a cubic structure. Electrical resistivity data (Fig. 2c) show a gradual decrease to *ca.* 750 K, followed by a more rapid decrease and then essentially constant behaviour above 800 K.

Rietveld refinement using the powder diffraction data collected at ambient temperature used, for the initial structural model, the lattice parameters and atomic coordinates for the tetragonal structure of chalcopyrite in space group $I\bar{4}2d$, reported by Hall and Stewart [27]. The neutron background was fitted using a reciprocal interpolation function with the coefficients included as refinable parameters, whilst the peak shape was modelled using a convolution of a Gaussian peak shape with a double exponential function within the GSAS software [25]. Weak reflections originating from boron nitride components within the sample cell were excluded where appropriate.

Simultaneous refinements using diffraction data collected in both backscattering and low-angle detector banks were performed, with the magnetic structure of $CuFeS_2$ determined by Donnay et al. [14] used as a starting model. The magnetic

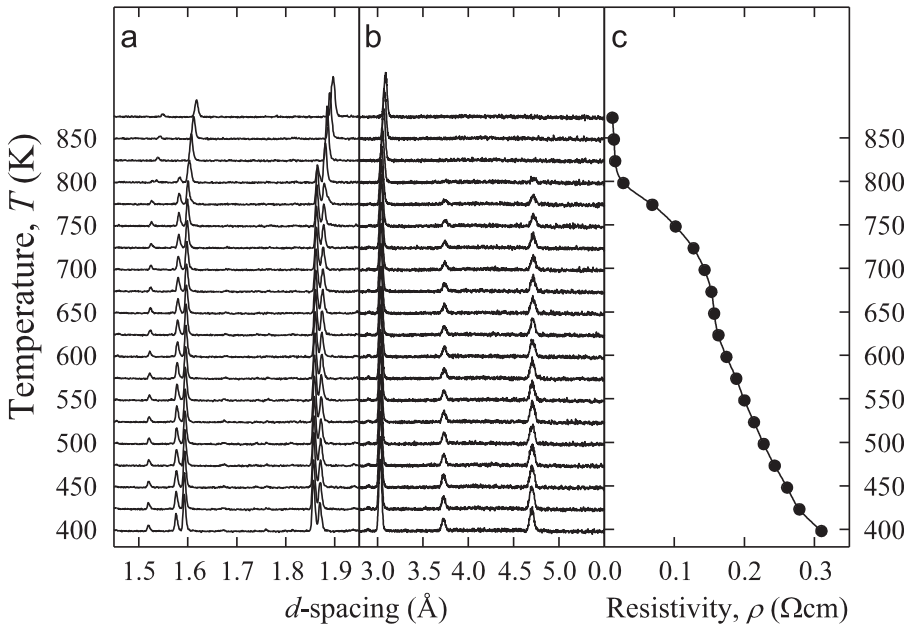

Fig. 2. A summary of the results of the in-situ neutron diffraction and electrical resistivity study of $CuFeS_2$ as a function of temperature. A portion of the diffraction pattern collected using (a) the backscattering and (b) low-angle detector banks is shown, together with (c) the temperature dependence of the resistivity of the sample.

structure was described in the primitive space group *P*1 and the free-ion form factor [28] for Fe^{3+} was used to describe the wavelength-dependence of the magnetic scattering. The data could be successfully fitted with localised moments associated with the iron cation only. The μ_x and μ_y components of the magnetic moment refined to values close to zero in the early stages of refinement and were subsequently fixed at this value, with μ_z being included as a variable in the refinement. In the resulting magnetic structure (Fig. 3), nearest-neighbour Fe^{3+} cations, which share a common sulphide tetrahedral vertex, are antiferromagnetically coupled. The Fe^{3+}–Fe^{3+} distance between tetrahedral centres is, at *ca.* 3.71 Å, too long for direct exchange through overlap of cation-based orbitals. Coupling between nearest neighbours is therefore of the superexchange type *via* the 108.6° Fe–S–Fe pathway, which for high-spin d^5 ions is predicted to be antiferromagnetic in origin. This results in a magnetic structure in which Fe^{3+} cations located in planes parallel to the (001) crystallographic plane are ferromagnetically aligned with one another and neighbouring planes of cations along the [001] direction are antiferromagnetically coupled. The observed magnetic moment μ(Fe) is 3.67(5) μ_B at 293 K. This value is intermediate between the value 3.85 μ_B reported by Donnay et al. [14] and 3.42(7) μ_B later determined by Woolley et al. [29] at the same temperature. The magnetic moment is considerably reduced from the spin-only value of 5 μ_B expected for a high-spin Fe^{3+}:d^5 cation. This reduction in moment was behind the early suggestion [14] of mixed valence states in $CuFeS_2$. However, given the spectroscopic confirmation of the presence of high-spin Fe^{3+}, it would appear that the reduction in the ordered moment of iron arises from spin-transfer from the cation as a result of the appreciable covalency of the Fe–S interaction.

Diffraction data collected with increasing temperature reveal that $CuFeS_2$ adopts the tetragonal chalcopyrite structure up to 748 K, with relatively little change in the degree of the tetragonal distortion (c/a) and no significant variations in the atomic parameters. The evolution of lattice parameters with temperature is provided as Supplementary Information. Sequential Rietveld refinement also allowed the evolution of the ordered magnetic moment to be investigated (Fig. 4) and a magnetic ordering temperature, T_N, of 823 K may be established from the variation of the magnetic moment with temperature. This is in excellent agreement with the previously reported value [12] derived from susceptibility data.

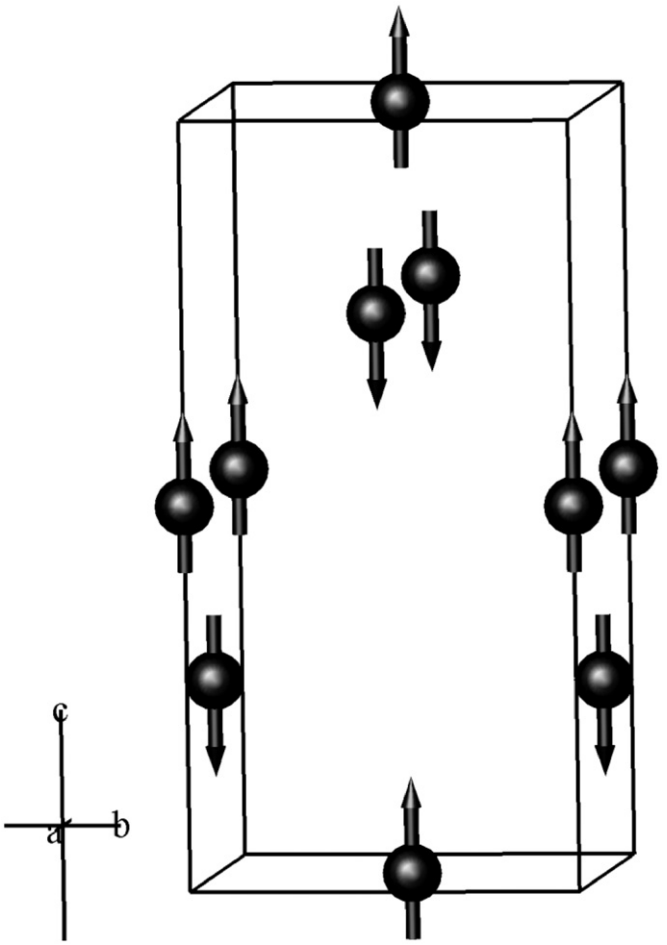

Fig. 3. The magnetic structure of $CuFeS_2$ at 293 K. Diamagnetic Cu^+ and S^{2-} ions are omitted for clarity.

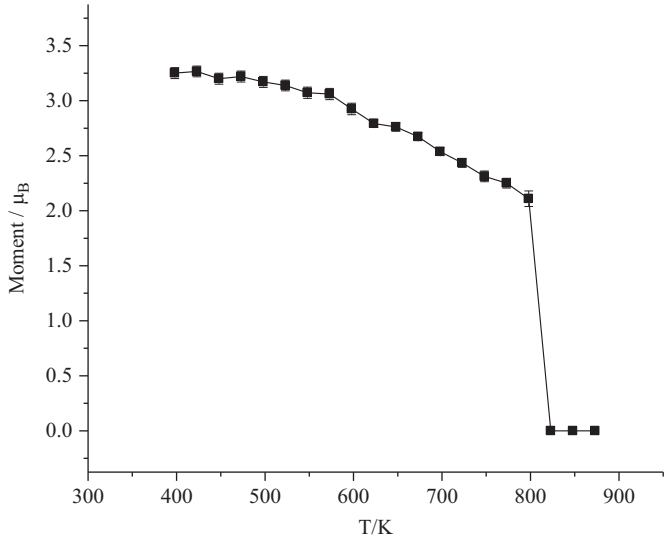

Fig. 4. The temperature dependence of the ordered moment of Fe^{3+} in $CuFeS_2$.

Table 1
Refined parameters for single-phase $CuFeS_2$ at selected temperatures, determined from simultaneous refinement against data collected in the backscattering and low-angle detector banks.

		293 K[a]	748 K[a]	823 K[b]
	a (Å)	5.2893(1)	5.3160(1)	5.3341(1)
	c (Å)	10.4278(2)	10.4721(3)	–
Cu	B (Å^2)	0.9(1)	3.4(2)	3.91(9)
Fe	Moment (μ_B)	3.67(5)	2.48(4)	–
	B (Å^2)	1.1(1)	2.4(1)	3.91(9)
S	x	0.248(6)	0.246(5)	–
	B (Å^2)	0.96(4)	3.0(1)	3.1(1)
R_{wp} (%)	145° bank	4.4	3.2	2.7
	35° bank	8.3	9.7	9.6
	χ^2	2.81	1.11	1.07

[a] Space group $I\bar{4}2d$: Cu on 4(a), (0, 0, 0); Fe on 4(b), (0, 0, 1/2); S on 8(d) (x, 1/4, 1/8).
[b] Space group: $F\bar{4}3m$: Cu and Fe on 4(a), (0, 0, 0) each with a site-occupancy factor of 0.5; S on 4(c) and (1/4. 1/4, 1/4) with a site-occupancy factor of 1.0.

The powder neutron diffraction data collected at temperatures of 773 and 798 K revealed the presence of two phases, identified as the tetragonal chalcopyrite phase (space group: $I\bar{4}2d$) and a cubic zinc blende structured phase (space group: $F\bar{4}3m$), in which there is a statistical occupancy of the single crystallographic 4(a) cation site by the copper and iron cations (Fig. 1a). Data at these temperatures required both phases to be included in the refinement in order to obtain a high-quality fit. Allowing the site-occupancy factor of sulphur to refine did not produce any statistically significant deviation from unity in either the tetragonal or cubic phases, and it was subsequently fixed at this value in all refinements using data collected at temperatures, $T \leq 798$ K. At higher temperatures, the data could be successfully fitted using the zinc blende structured phase alone, indicating that the loss of magnetic order is coincident with the completion of the transformation to the cubic structure. Although refinement of the site-occupancy factor of sulphur at 823 K on heating, provides some indication of sulphur deficiency, the parameter is strongly correlated with the thermal parameter of sulphur and its absolute value is therefore unreliable. For this reason the refined parameters reported in Table 1 are for the fully stoichiometric phase, for which there is no discernable difference in the goodness-of-fit parameters compared to the non-stoichiometric phase. Representative final observed, calculated, and difference profiles at temperatures of 293 K (tetragonal phase), 748 K (immediately below the two-phase region), 798 K (in the two phase region), and 823 K (cubic phase) are given in Figs. 5 and 6 and the final refined parameters for the single phase regions are presented in Table 1. Significant bond lengths and angles are provided in Table 2.

The electrical resistivity data are consistent with semiconducting behaviour (Fig. 2c) throughout the temperature range investigated. The slight change in $d\rho/dT$ in the region of 600 K is not reflected in any structural change detectable by neutron diffraction. It may be identified with a similar decrease in resistivity at 573 K reported by Teranishi [12] and in a similar manner can be attributed to a change from extrinsic (impurity) to intrinsic conduction. In common with other workers, we did not observe the increase in resistivity with rising temperature at 773 K reported by Boltaks and Tarnovskii [13]. Instead, the data measured using the *in-situ* conductivity cell shows that $CuFeS_2$ exhibits a significant decrease in resistivity, starting at around 740 K and continuing until a temperature of approximately 823 K, above which it remains essentially independent of temperature. We can associate this decrease in resistivity with the onset of the cation disorder within the $CuFeS_2$ structure, as indicated by the two-phase region identified by the analysis of the diffraction data: the resistivity of the fully disordered phase then remains effectively constant once the structural phase transition is complete. The origin of the decrease in resistivity is likely to lie in changes in band structure as a result of cation disorder associated with a change to a more symmetric structure.

The sample recovered from the diffraction-resistance cell after cooling to room temperature from the highest temperature reached during the experiment (873 K) was black in appearance. Neutron diffraction data collected on cooling were well fitted by the cubic structural model at all temperatures. No reversion to the tetragonal structure was evident, although a plot of the cubic lattice parameter as a function of temperature (Fig. 7) exhibits a maximum at *ca.* 800 K, the region in which on heating, cubic and tetragonal phases co-exist. The irreversible nature of the phase transition was reflected in the irreproducibility in the resistivity behaviour upon cooling. The origin of these observations may lie in the loss of sulphur from the sample at the highest temperature of 873 K reached in this investigation. Although the sample was prepared at elevated temperatures in an evacuated sealed silica tube (approximate volume 11 cm^3), volatilization of sulphur during synthesis is, in the absence of temperature gradients, fully reversible on slow cooling. By contrast, the *in-situ* diffraction-resistance cell has a much larger volume (*ca.* 500 cm^3), contains a number of components and temperature gradients are present. Whilst it is sealed under a reduced pressure during operation, temperature gradients result in sulphur preferentially condensing on the cooler components, leading to irreversible removal of sulphur from the sample at temperatures above the structural phase transition. Furthermore, discolouration of some surfaces suggests that sulphur vapour may also react with platinum components under these conditions. The irreversible loss of sulphur is supported by refinement of the site-occupancy factor for the sulphur 4(c) site in the cubic zinc blende phase on cooling from 873 K. The site-occupancy factors of the 4(c) site after heating to 873 K show a significant deviation from unity to values of *ca.* 0.87, albeit with the proviso concerning correlation noted above, that is consistent with the evaporation of sulphur from the sample pellet at high temperature. There was no evidence for elemental sulphur in the diffraction pattern of the pellet after cooling to room temperature, as expected if deposition on the components of the diffraction-resistance cell has occurred. The

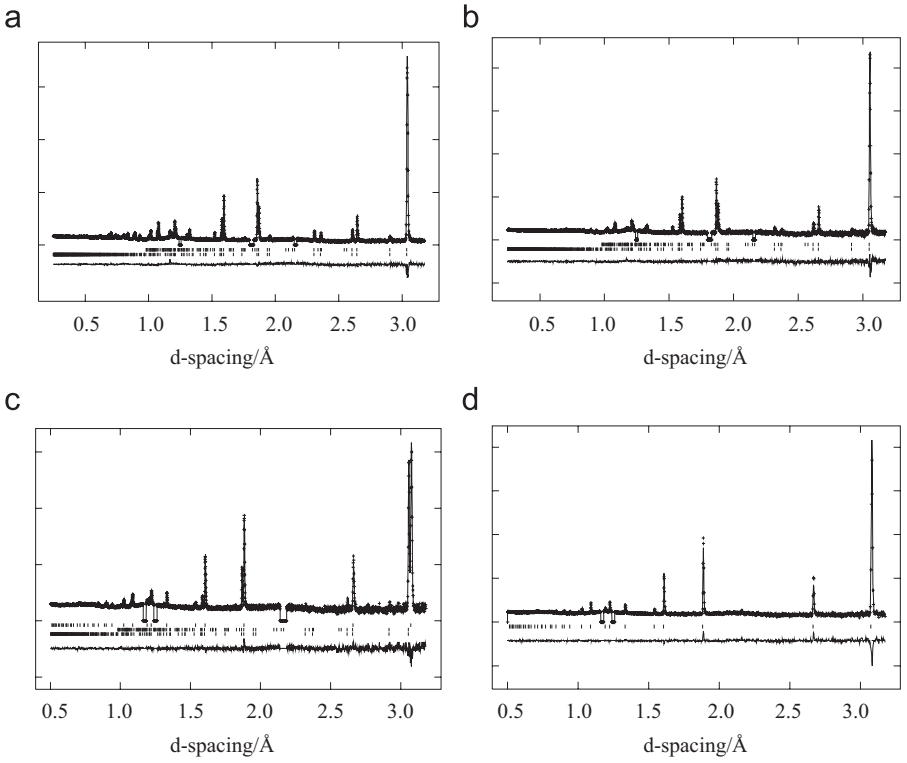

Fig. 5. Final observed (crosses), calculated (full line) and difference (lower full line) neutron profiles for the backscattering detector bank ($2\theta = 145^{\circ}$) at (a) 293 K, (b) 748 K, (c) 798 K and (d) 823 K. Reflection positions are marked: in (a)–(c) the lower markers refer to the crystallographic unit-cell (space group: $I\bar{4}2d$) and the upper markers refer to the magnetic unit-cell described in the primitive space-group $P1$. The markers in (d) refer to the cubic phase (space group: $F\bar{4}3m$) as do the middle markers in (c). Excluded regions correspond to scattering from BN components of the *in-situ* cell.

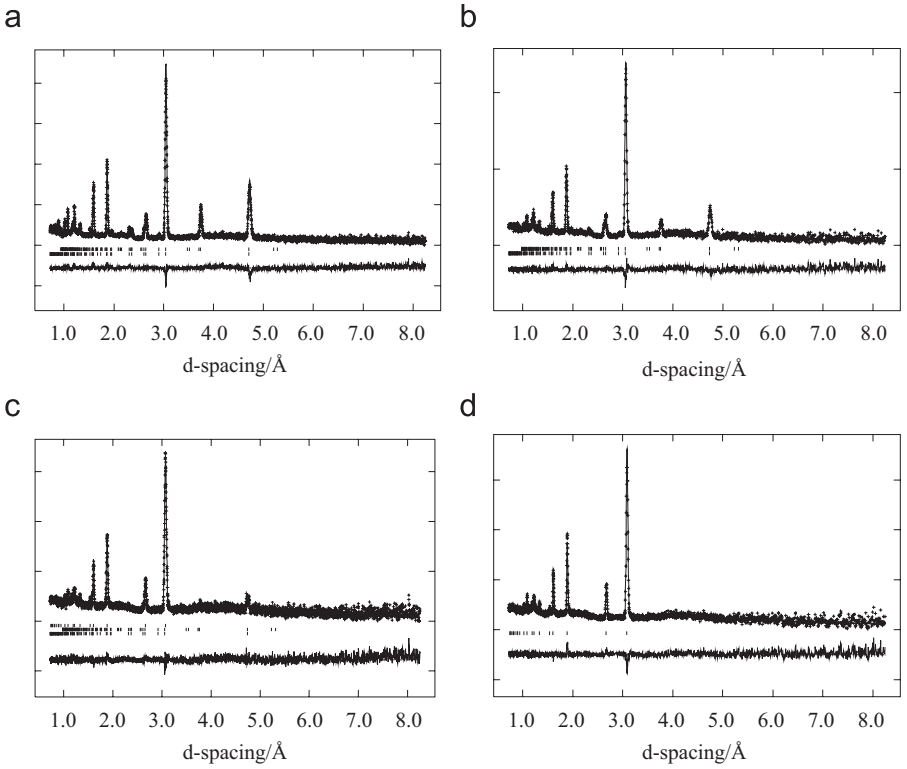

Fig. 6. Final observed (crosses), calculated (full line) and difference (lower full line) neutron profiles for the low-angle detector bank ($2\theta = 35^{\circ}$) at (a) 293 K, (b) 748 K, (c) 798 K and (d) 823 K. Reflection positions are marked: in (a)–(c) the lower markers refer to the crystallographic unit-cell (space group: $I\bar{4}2d$) and the upper markers refer to the magnetic unit-cell described in the primitive space-group $P1$. The markers in (d) refer to the cubic phase (space group: $F\bar{4}3m$) as do the middle set of markers in (c).

Table 2
Selected bond distances (Å) and angles (°) for $CuFeS_2$ in the tetragonal and cubic forms.

Tetragonal phase at 293 K		Cubic phase at 848 K	
Cu–S	$4 \times 2.272(18)$	M–S	$4 \times 2.31633(3)$
Fe–S	$4 \times 2.287(18)$	M–M	$12 \times 3.78255(4)$
Fe–Fe	$4 \times 3.7136(1)$	S–M–S	$6 \times 109.471(1)$
Cu–Fe	$4 \times 3.7136(1)$		
	$4 \times 3.7401(1)$		
S–Cu–S	$4 \times 109.2(3)$		
	$2 \times 110.0(6)$		
S–Fe–S	$4 \times 108.9(3)$		
	$2 \times 110.5(6)$		

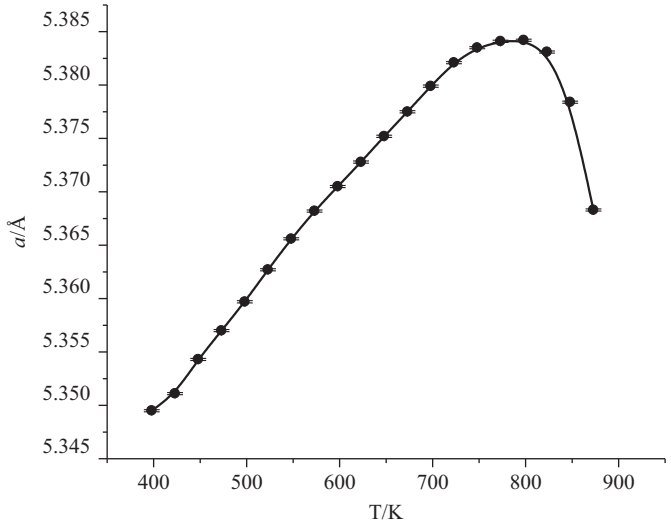

Fig. 7. Variation in the cubic lattice parameter on cooling the sample in the in-situ diffraction-resistance cell from 873 K.

loss of sulphur at elevated temperatures is in agreement with the observation of Frueh [30] who reported that as $CuFeS_2$ is heated; it loses sulphur and there is a concomitant irreversible decrease in resistivity. It has been suggested [21] that at temperatures above 823 K, $CuFeS_2$ undergoes decomposition to pyrite plus a disordered, face-centred-cubic phase, close in composition to chalcopyrite. However, the diffraction data collected in the course of this work could be successfully fitted using the cubic zinc blende phase, even at the highest temperature, with no evidence of any pyrite-type phase.

4. Conclusions

In conclusion, through measurements of resistivity, simultaneously with the collection of powder neutron diffraction data as a function of temperature, we have investigated the relationship between the structural, magnetic and electron-transport properties of $CuFeS_2$ in a single experiment. The results demonstrate that on heating the onset of cation disorder within the ordered chalcopyrite precedes the loss of long-range antiferromagnetic order and that at T_N, complete conversion to the fully disordered cubic zinc blende type phase occurs. Furthermore, the data reveal that the anomaly in $\rho(T)$ behaviour observed at *ca.* 600 K is not structural in origin, supporting the view that it is associated with a change from extrinsic to intrinsic conduction. By contrast however, the reduction in resistivity that begins at 740 K appears to be associated with the onset of the tetragonal to cubic phase transition, as evidenced by the co-existence of tetragonal and cubic phases at 773 and 798 K. The data also provide evidence that the loss of sulphur at elevated temperatures can lead to irreversibility in the structural, magnetic and electronic phase transitions.

Acknowledgments

Erinc Engin thanks Heriot-Watt University and the STFC Centre for Materials, Physics and Chemistry for the financial support during his PhD studentship.

Appendix A. supplementary material

Supplementary data associated with this article can be found in the online version at doi:10.1016/j.jssc.2011.06.036.

References

[1] D.J. Vaughan, J.R. Craig, Mineral Chemistry of Metal Sulphides, Cambridge University Press, Cambridge, 1978.
[2] T. Teranishi, K. Sato, K. Kondo, J. Phys. Soc. Jpn. 36 (1974) 1618.
[3] S.C. Erwin, I. Žutic, Nat. Mater. 3 (2004) 410.
[4] S. Chen, X.G. Gong, A. Walsh, S.-H. Wei, Phys. Rev. B 79 (2009) 165211.
[5] G.A. Medvedkin, T. Ishibashi, T. Nishi, K. Hayata, Y. Hasegawa, K. Sato, Jpn. J. Appl. Phys. 39 (2000) L949.
[6] Y.-J. Zhao, P. Mahadevan, A. Zunger, Appl. Phys. Lett. 84 (2004) 3753.
[7] A.A. Rockett, Curr. Opin. Solid State Mater. Sci. 14 (2010) 143.
[8] M.G. Panthani, V. Akhavan, B. Goodfellow, J.P. Schmidtke, L. Dunn, A. Dodabalapur, P.F. Barbara, B.A. Korgel, J. Am. Chem. Soc. 130 (2008) 16770.
[9] Q. Guo, S.J. Kim, M. Kar, W.N. Shafarman, R.W. Birkmire, E.A. Stach, R. Agrawal, H.W. Hillhouse, Nano Lett. 8 (2008) 2982.
[10] C. Pearce, R.A.D. Patrick, D.J. Vaughan, Rev. Miner. Geochem. 61 (2006) 127.
[11] L. Barkat, N. Hamdadou, M. Morsli, A. Khelil, J.C. Bernède, J. Cryst. Growth 297 (2006) 426.
[12] T. Teranishi, J. Phys. Soc. Jpn. 16 (1961) 1881.
[13] B.I. Boltaks, N.N. Tarnovskii, Zh. Tekh. Fiz. 25 (1955) 402.
[14] G. Donnay, L.M. Corliss, J.D.H. Donnay, N. Elliot, J. Hastings, Phys. Rev. 112 (1958) 1917.
[15] L. Pauling, L.O. Brockway, Z. Krist. 82 (1932) 188.
[16] C. Boekema, A.M. Krupski, M. Varasteh, K. Parvin, F. van Til, F. van der Woude, G.A. Sawatzky, J. Magn. Magn. Mater. 272–276 (2004) 559.
[17] H.N. Ok, K.S. Baek, E.J. Choi, Phys. Rev. B 50 (1994) 10327.
[18] E.Z. Kurmaev, J. van Ekt, D.L. Ederer, L. Zhou, T.A. Callcott, R.C.C. Perera, V.M. Cherkashenko, S.N. Shamin, V.A. Trofimova, S. Bartowski, M. Neumann, A. Fujimori, V.P. Moloshag, J. Phys. Condens. Matter 10 (1998) 1687.
[19] Y. Mikhlin, Y.V. Tomashevich, V. Tauson, D.V. Vyalikh, S. Molodtsov, R. Szargan, J. Electron. Spectrosc. Relat. Phenom. 142 (2005) 83.
[20] C.I. Pearce, R.A.D. Patrick, D.J. Vaughan, C.M.B. Henderson, G. van der Laan, Geochim. Cosmochim. Acta 70 (2006) 4635.
[21] J.E. Hiller, K. Probsthain, Z. Krist. 108 (1956) 108.
[22] L.J. Cabri, Econ. Geol. 68 (1973) 443.
[23] R. Adams, P. Russo, R. Arnott, A. Wold, Mater. Res. Bull. 7 (1972) 93.
[24] S. Hull, R.I. Smith, W.I.F. David, A.C. Hannon, J. Mayers, R. Cywinski, Physica B 180–181 (1992) 1000.
[25] T.E. Engin, A.V. Powell, R. Haynes, M.A.H. Chowdhury, C.M. Goodway, R. Done, O. Kirichek, S. Hull, Rev. Sci. Instrum. 79 (2008) 095104.
[26] A.C. Larson, R.B. von Dreele, Los Alamos National Laboratory Report, 1994, LAUR 86–748.
[27] S.R. Hall, J.M. Stewart, Acta Cryst. B 29 (1973) 579.
[28] P.J. Brown, in: A.J.C. Wilson (Ed.), International Tables for Crystallography, Vol. C., Kluwer, Dordrecht, 1992 Chapter 4.
[29] J.C. Woolley, A.M. Lamarche, G. Lamarche, M. Quintero, I.P. Swainson, T.M. Holden, J. Magn. Magn. Mater. 162 (1996) 347.
[30] A.J. Frueh, Am. Min. 44 (1959) 1010.